

1 **GOSML: A Global Ocean Surface Mixed Layer Statistical Monthly Climatology:**
2 **Means, Percentiles, Skewness, and Kurtosis**

3
4 Gregory C. Johnson¹

5 John M. Lyman^{1,2}

6 ¹*NOAA/Pacific Marine Environmental Laboratory, Seattle, Washington 98115, USA*

7 ²*CIMAR/University of Hawaii, Honolulu, HI 96822, USA*

8
9 for *Journal of Geophysical Research*

10 Submitted 5 November 2021, revised 6 January 2022, accepted 12 January 2022

11 <https://doi.org/10.1029/2021JC018219>

12 **Key points:**

- 13 • A monthly climatology of mixed layer property means, variances, percentiles (5th, 50th,
14 and 95th), skewness, and kurtosis is analyzed
- 15 • Mixed layer depth 95th percentiles, reasonable ventilation indicators, substantially exceed
16 mean values at many locations and times
- 17 • Mixed layer properties are not normally distributed, with depths often positively skew,
18 especially between late spring and early summer

19
20 **Index Terms:** 4572 Upper ocean and mixed layer processes; 4227 Diurnal, seasonal, and annual
21 cycles; 4223 Descriptive and regional oceanography; 3252 Spatial analysis; 4262 Ocean
22 observing systems

23 **Keywords:** Ocean Surface Mixed Layer; Argo; Statistics; Skewness; Kurtosis; Global Ocean

25 **Abstract** Here we discuss a global ocean surface mixed layer statistical monthly climatology
26 (GOSML) of depth, temperature, and salinity that includes means; variances; 5th, 50th, and 95th
27 percentiles; as well as skewness and kurtosis. Ocean surface mixed layer properties are
28 influenced by gravity and a wide variety of factors that operate over a wide variety of time
29 scales. Mixed layer depths can shoal very quickly as a result of surface heating, precipitation, or
30 “slumping” of horizontal density gradients. However, deepening the mixed layer in the presence
31 of a strong pycnocline requires substantial buoyancy loss or strong wind mixing, which often
32 takes more time. This pattern is clear in the annual cycle monthly mixed layer depth values, with
33 deepening in the fall much slower than shoaling in the spring. The 95th percentile values are
34 chosen as a reasonable indicator of ventilation depth, robust to extreme outliers. Mean mixed
35 layer depths are on average 0.56 of 95th percentile mixed layer depths, with only 1% of values
36 below 0.31 and 1% above 0.81. Over 71% of mixed layer depth distributions are skewed
37 positive, usually when there are more shallow mixed layer depths than not and deep mixed layer
38 tails are strong. Comparing 95th percentile depth conditions to mean values shows in late winter
39 temperatures are generally lower in the subtropics and salinities generally higher in the subpolar
40 regions, consistent with the importance of temperature in the midlatitudes and salinity in the
41 higher latitudes in setting stratification.

42 **Plain Language Summary** The ocean surface mixed layer is key to exchanges of heat,
43 freshwater, momentum, and dissolved gasses between atmosphere and ocean. Hence, it affects
44 marine life, weather, and climate. Mixed layer depths shoal suddenly with warming from the sun,
45 rainfall, riverine outflow, or currents that slide lighter water over denser. However, mixed layer
46 deepening requires loss of heat or freshwater to the atmosphere or strong wind mixing to
47 overcome ocean density stratification below. The monthly mixed layer climatology presented
48 here illustrates that asymmetry, with slow deepening from summer to winter, and fast shoaling
49 during the spring. Likewise, shallower mixed layers often predominate over deeper ones for
50 many months and locations. Since the deeper mixed layers determine the local exchange of
51 surface properties with the ocean interior (known as ventilation), mean values are not a good
52 indicator of those processes. Here we choose 95th percentile mixed layer depths in a given month
53 (and the associated temperature and salinity values) as an indicator of the ventilation conditions
54 that is not impacted by extreme outliers. These 95th percentile depths are on average about 85%
55 deeper than the means, but can reach over five times deeper in a few locations at a few times.
56

57 **1. Introduction**

58 Ocean surface mixed layer (hereafter mixed layer) dynamics are asymmetrical, as is visible even
59 on diurnal time scales (Price et al., 1986). Pronounced mixed layer shoaling can occur relatively
60 rapidly, through buoyancy gains by surface heating (Price et al., 1986), surface precipitation
61 (Sprintall & Tomczak, 1992), riverine input (Rao & Sivakumar, 2003), or ice melt (Vernet et al.,
62 2008); through advection via “slumpling” of horizontal density gradients in the mixed layer
63 (Boccaletti et al., 2007); or some combination thereof. In other words, it is easy for mixed layer
64 depth to shoal rapidly and drastically, especially in low wind conditions. On the other hand, in
65 order to deepen, the surface mixed layer has to become denser and mix through an underlying
66 stratified pycnocline, which requires buoyancy losses by surface cooling, evaporation, or ice
67 formation; wind mixing; or some combination thereof. Hence, it typically takes more time for a
68 mixed layer to deepen than to shoal (Damerell et al., 2020). This asymmetry suggests that mixed
69 layer properties (e.g., depth, temperature, salinity, and density) may not be normally distributed.
70 Nonetheless, many (de Boyer Montegut et al., 2004; Kara et al., 2003), although not all (Holte et
71 al., 2017) mixed layer climatologies are computed from averages of data distributions, which
72 assume a normal distribution.

73

74 Mixed layer properties are determined by surface fluxes of buoyancy (e.g., heat and freshwater),
75 and kinetic energy (e.g., wind) (Price et al., 1986) that all vary on time scales from minutes to
76 hours (microscale weather), hours to days (mesoscale weather and the diurnal cycle), days to
77 weeks (synoptic-scale weather), weeks to months (global-scale weather and the seasonal cycle),
78 and months to millennia (climate variations). This wide range of time scales for interactions

79 between the ocean surface mixed layer and the atmosphere also suggests that mixed layer
80 properties may not be normally distributed.

81

82 Means and variances are especially useful for describing normal distributions. Here, because of
83 the issues discussed above, we present additional statistics for mixed layer properties (depth, and
84 also temperature and salinity), including the median (50th percentile), 5th, and 95th percentiles.
85 We chose the 95th percentile of the depth distribution for a given location and month as a
86 reasonable indicator of the depth to which the ocean is ventilated on seasonal time scales. While
87 this choice is similar in intent to the average of the three deepest values (Holte et al., 2017), it is
88 more independent of the number of samples taken (the average of the deepest three values could
89 be very different when considering 3000 samples versus 30, but the 95th percentile remains
90 constant in meaning) and more robustly excludes extreme outliers. We also include the 5th
91 percentile of the depth distribution for a given location and month to illustrate the mixed layer
92 properties at times when it is lighter and shallower. Finally, we present and discuss the skewness
93 (the third standardized moment of a distribution, which typically indicates which side of the
94 distribution has a larger tail), and kurtosis (the fourth standardized moment of a distribution,
95 which indicates the prominence of the tails of the distribution) of mixed layer properties.

96

97 Argo floats have been collecting vertical profiles of temperature and salinity versus pressure
98 from the ocean surface to pressures of 2,000 dbar since the inception of the program around the
99 turn of the millennium (Johnson et al., 2022). These publicly available data, collected globally
100 and year-round, allow a more detailed examination of monthly ocean surface mixed layer
101 statistics. Here we estimate the mean, variance, skewness, and kurtosis for mixed layer depth,

102 temperature, salinity, and density, as well as 5th, 50th, and 95th percentiles of mixed layer
103 properties sorted by depth and then smoothed.

104

105 **2. Data and Methods**

106 Argo data were downloaded from the US Global Data Assembly Centre in January 2021
107 (<https://doi.org/10.17882/42182>). Only data with quality flags of 1 (good) or 2 (probably good)
108 were used. Adjusted fields (delayed-mode scientific quality controlled) were used where
109 available, and unadjusted fields (real-time automated quality controlled) were used otherwise.

110

111 Mixed layer properties (average temperature, practical salinity, and depth) were determined from
112 each Argo profile using the density algorithm of Holte & Talley (2009). With its relatively
113 sensitive thresholds and use of temperature and salinity data, this algorithm is well suited to the
114 Argo data set. Following that the absolute salinity, conservative temperature, and potential
115 density were calculated using the 2010 equation of state (TEOS-10) for seawater (Feistel, 2012).

116

117 A monthly climatology of mixed layer properties was estimated using the following methods:

118 The data were analyzed on a global grid with resolution of one month in time, 1° in latitude, and
119 1° in longitude. Bottom depth values were set for each mixed layer estimate and the grid
120 locations through linear interpolation of ETOP01 bathymetry data (Smith & Sandwell, 1997) that
121 had been smoothed with a 30' (latitude and longitude) half-width Hanning filter and subsampled
122 at 15' intervals. For each point a loess weighting (Cleveland & Devlin, 1988) w was constructed
123 with a 1-month time scale, a 500-km length scale, and a bottom depth weighting as follows:

$$124 \quad q = \left| \frac{y_g - y_f}{4.521^\circ} \right| + \left| \frac{(x_g - x_f) \times \cos(y_g)}{4.521^\circ} \right| + \left| \frac{t_g - t_f}{1 \text{ month}} \right| + \frac{1}{\log(10)} \times \left| \log \left(\frac{h_g}{h_f} \right) \right| \quad (1)$$

125 where y is longitude, x is latitude (both in degrees), t is time (in months), h is bottom depth (in
126 meters), the subscript g indicates the grid points, and the subscript f the individual floats, and

$$127 \quad w = (1 - q^3)^3 \text{ for } q < 1 \text{ and } w = 0 \text{ for } q \geq 1. \quad (2)$$

128 The length scales for the weighting are chosen to emphasize large-scale distributions and to
129 match the nominal Argo 3° sampling, the time scale is set to resolve the seasonal cycle, and the
130 bottom depth weighting serves to separate grid points in the open ocean, the continental slopes,
131 and the shelves.

132
133 At each grid point the data selected are first screened for really extreme outliers, rejecting data
134 points with mixed layer depths, temperatures, or salinities that are 6 times the interquartile range
135 greater than the 75th percentiles or 6 times less than the 25th percentiles. (These outliers can result
136 from bad data points that have escaped quality control or very non-normal property distributions
137 of valid data. On average, outliers comprise < 0.2% of the total number of points used in the
138 mapping. Of the grid points mapped, 92% contain no outliers, 5% contain more than 1% outliers,
139 and only 0.4% contain more than 10% outliers.) After removing outliers, the weighted mean,
140 variance, skewness, and kurtosis are calculated for mixed layer depth, absolute salinity,
141 conservative temperature, and potential density using the remaining points.

142
143 Skewness, $Skew(x)$, at a grid point for a variable x is defined as

$$144 \quad Skew(x) = \frac{\sum[(x_i - \bar{x})^3 \cdot w_i]}{\sigma^3 \cdot \sum w_i}, \quad (3)$$

145 where x_i is the variable in question for a given sample i , w_i is the weight of that sample as
146 defined in (1) and (2), \bar{x} is the weighted mean at the grid point, and σ is the weighted standard
147 deviation at the grid point. Skewness is a signed quantity that is generally positive when the

148 distribution has a stronger tail on the right side and negative when the distribution has a stronger
149 tail on the left side.

150

151 Similarly, kurtosis, $Kurt(x)$, at a grid point for that same variable x is defined as

$$152 \quad Kurt(x) = \frac{\sum[(x_i - \bar{x})^4 \cdot w_i]}{\sigma^4 \cdot \sum w_i}. \quad (4)$$

153 In contrast to skewness, kurtosis is a positive definite quantity. $Kurt(x) = 3$ for a normal
154 distribution. When $Kurt(x) < 3$ the distribution has small tails. When $Kurt(x) > 3$ the distribution
155 has large tails.

156

157 Retained data for all four variables used at each grid point are then sorted by mixed layer depth
158 to find 5th, 50th, and 95th percentile values at those depths. They are smoothed in percentile space
159 with a weighted local linear fit, a lowess filter (Cleveland & Devlin, 1988), with a length scale of
160 25% of the sorted, weighted distribution. The weighting used is the product of the distance in this
161 depth-sorted percentile space and the geographic distance/time/bottom depth weighting of the
162 data point from the grid point weighting described in (1). Smoothed 5th, 50th (median), and 95th
163 percentile values are determined for all four variables.

164

165 **3. Results**

166 This section has four subsections. Firstly, we discuss the number of points used in each map, and
167 the weighted number (i.e., the effective number) of points. Secondly, we move onto looking at
168 seasonal cycles of mixed layer properties (depth, temperature, and salinity; their means; and
169 values at the 5th, 50th, and 95th percentile mixed layer depths) in four locations where prominent
170 mode waters are formed. These are the Labrador Sea where Labrador Sea Water (LSW) is

171 formed by deep convection (Yashayaev & Loder, 2016), the western North Atlantic subtropical
172 gyre, where Eighteen Degree Water (EDW) is formed by subduction (Billheimer & Talley,
173 2016), the subantarctic Southeast Pacific, where the most extreme form of SubAntarctic Mode
174 Water (SAMW) is formed by subduction (Sallée et al., 2010), and the eastern subtropical South
175 Pacific, where South Pacific Eastern SubTropical Mode Water (SPESTMW) is formed by
176 subduction (Wong & Johnson, 2003). Thirdly, we discuss the mixed layer properties sorted by
177 mixed layer depth around the time of maximum mixed layer depths (mid-March and mid-
178 September; late winter and late summer depending on hemisphere) in these regions. We also
179 discuss mid-March and mid-September 95th percentile mixed layer depths globally, as well as
180 their ratios to the mean depths. In addition, we discuss the differences between temperature and
181 salinity at the 95th percentile in depth to the means in terms of whether warmer or colder and
182 saltier or fresher conditions are associated with 95% percentile mixed layer depths relative to the
183 mean properties. Fourthly, we discuss higher order moments (skewness and kurtosis) of the
184 mixed layer properties, focusing on mixed layer depths during the transition months of mid-May
185 and mid-November, when their regional patterns are most pronounced. While the number of
186 figures in the article is limited, the climatology itself and global maps of seasonal cycles of all of
187 these fields are available at <https://www.pmel.noaa.gov/gosml>.

188

189 *3.1 Data Distribution and Number of Data Used*

190 While the data are generally evenly distributed throughout the year, there is considerable
191 geographic variation in the sampling density, even for Argo. The most sampled regions are in the
192 North Atlantic, North Pacific, and North Indian oceans with the number of data points used in
193 March (Figure 1a) exceeding 500 in a few regions as well as other months (not shown) and the

194 sum of the sample weights (Figure 1b) exceeding 100. There are only small regions where the
195 number of points used falls below 50, or the sum of the sample weights falls below 10.

196

197 The sum of the weights for the grid points is on average about $\frac{1}{4}$ of the sum of the number of
198 samples used at each grid point. The mean sum of the number of samples for grid points is 122
199 and the median is 111. About 5% of the grid points have a number of samples exceeding 242 and
200 5% of the grid points have a number of samples less than 36. If the number of samples originally
201 selected for a given grid point is less than 20, statistics there are not computed, to ensure at least
202 a minimal basis for the 5th and 95th percentile values reported. The mean sum of the weights for
203 grid points is 30 and the median is 27. About 5% of the grid points have a sum of the weights
204 exceeding 62 and about 5% of the grid points have a sum of the weights less than 8.

205

206 *3.2 Seasonal Cycles at Select Mode Water Formation Regions*

207 The seasonal cycles of mixed layer depth, temperature, and salinity (Figure 2), in a few select
208 locations (see magenta pentagrams in Figure 1a) show distinct patterns. We choose the cores of
209 formation for the LSW in the Labrador Sea, the EDW in the western subtropical North Atlantic,
210 the SPESTMW in the eastern subtropical South Pacific, and the most extreme (coldest and
211 freshest, and close to thickest) variety of SAMW in the Southeast Pacific.

212

213 In the center of the Labrador Sea, where LSW is formed, the mixed layer depth (Figure 2a) is a
214 maximum in March, with cold temperatures (Figure 2e), and relatively salty (Figure 2i)
215 conditions in that month. The 95th percentile mixed layer depths in winter are considerably larger
216 than the mean or the median values. The mean values exceed the median values considerably in

217 the winter and early spring, when very deep mixed layer depths are episodically present. The 5th
218 percentile values are relatively shallow throughout the year, reflecting the fact that temporary
219 shallow mixed layers can form in calm conditions year-round through either freshening or
220 warming. Mixed layer depths at this location are relatively shallow from June until November
221 with a minimum in August (around 35 m at the 95th percentile), deepen rapidly from December
222 to February with a maximum in March (around 1760 m at the 95th percentile), and then shoal
223 very rapidly from April to May. In contrast mixed layer temperatures and salinities are relatively
224 cold and salty from December through April (with a March minimum of 3.2 °C and a maximum
225 of 35.02 g kg⁻¹ at the 95th percentile), warm and freshen steadily from April through August
226 (with an August maximum of 9.3 °C and a September minimum of 34.66 g kg⁻¹ at the 95th
227 percentile), and then cool and salinify relatively steadily from August (or September) through
228 November. The 5th percentile mixed layer salinity values are generally fresher than the 95th
229 percentile values, with the means and medians very similar and in between. The 95th percentile
230 temperature values are colder than the 5th percentile values except in the winter months, when
231 that tendency reverses. As for salinity, the 5th percentile values are fresher than the 95th percentile
232 values, with the mean and median values generally between, but approaching the 5th percentile
233 values in summer (as detailed above, the 5th and 95th percentile temperature and salinity values
234 were sorted by depth and then smoothed prior to evaluation).

235

236 Moving from the subpolar to the western subtropical mode waters of the North Atlantic, where
237 EDW is formed, the mixed layer depth patterns follow a similar seasonal cycle, but with a muted
238 amplitude. The March maximum of the 95th percentile depth values reaches 500 m, and the July
239 minimum is about 42 m (Figure 2b). The late winter and early spring mean depths are again

240 larger than the median depths, but the spring shoaling is less rapid, with the bulk taking place
241 from March through May, so starting a month earlier than further north. Mixed layer
242 temperatures (Figure 2f) and salinities (Figure 2j) are again relatively cold and salty during
243 winter months with a 95th percentile temperature minimum of 17.9 °C in March (fitting for
244 EDW) and a 95th percentile maximum salinity of 36.75 g kg⁻¹ in January. Temperatures rise
245 fairly steadily from May through August, reaching a maximum value of 27.0 °C in August, then
246 fall steadily from August through December. Salinity follows a similar (although opposite in
247 sign, hence reinforcing each other in their effect on mixed layer density) pattern to temperature,
248 with a 95th percentile value minimum of 36.40 g kg⁻¹ in August. The 5th percentile salinity values
249 are often substantially fresher than the 95th percentile values, indicating the role of surface
250 freshening in mixed layer shoaling in the region.

251
252 Moving to the Southern Hemisphere, in the Southeast Pacific where the winter mixed layers are
253 deepest and the most extreme form of SAMW is produced, the 95th percentile mixed layer depth
254 (Figure 2c) reaches a minimum of about 92 m in January and a maximum of 611 m in
255 September. Most of the mixed layer shoaling takes place from October to November, and the
256 deepening from April to August. Hence, there is substantial seasonal asymmetry, with faster
257 shoaling than deepening, like in the Labrador Sea. The mean and median mixed layer depth
258 values are generally pretty similar. The 5th percentile mixed layer depth is relatively deep
259 compared to the Labrador Sea, reaching a maximum around 121 m in July, suggesting that fresh
260 or warm caps are comparatively infrequent in this portion of the Southeast Pacific in fall and
261 winter. The summer warm period is also pretty short (Figure 2g), with a 95th percentile
262 temperature value maximum of 6.8 °C in January, and the winter cold period is pretty long, from

263 about May through November, with a minimum 95th percentile temperature of 5.4 °C in
264 September. The 5th percentile mixed layer temperature is warmer than the 95th, with the mean
265 and median similar and in between, except in the dead of winter, when all values are quite
266 similar. The mixed layer salinity distribution (Figure 2k) is more sinusoidal than the temperature,
267 with a maximum 95th percentile salinity of 34.37 g kg⁻¹ in August and a salinity minimum of
268 34.24 g kg⁻¹ in February. The 5th percentile salinity is often considerably fresher than the 95th
269 percentile salinity, again stressing the importance of fresher surface conditions during periods of
270 shallower mixed layers. In this case some of that variability is likely to be spatial, as the surface
271 mixed layer gets fresher and shallower toward the south within 500 km of this location.

272

273 Finally, in the heart of the SPESTMW formation in the Southeast Pacific, 95th percentile mixed
274 layer depth values (Figure 2d) reach a maximum of 218 m in August, and a minimum of 55 m in
275 February. The mean and median values of mixed layer depth are fairly similar to each other.
276 Again, the 5th percentile mixed layer depth values are larger than in the Northern Hemisphere
277 subtropical EDW formation region, reaching maximum values of 64 m in July. Mixed layers
278 deepen from March to August and shoal, more rapidly, from September to December. The
279 annual harmonic is strong in the mixed layer temperature seasonal cycle here (Figure 2h), with a
280 95th percentile (again, in terms of sorted weighted depths) maximum of 25.0 °C in March and a
281 minimum of 20.7 °C in August. The 5th percentile temperature values are generally warmer than
282 the 95th percentile values, especially in austral winter, with mean and median values fairly
283 similar and in between the 5th and 95th percentile values. The mixed layer salinity values are also
284 sinusoidal in character (Figure 2l), with a maximum 95th percentile value of 36.77 g kg⁻¹ in
285 March and a minimum of 36.22 g kg⁻¹ in August. The seasonal cycle of salinity values at 5th

286 percentile depth mixed layers is muted compared to that for the 95th percentile depth mixed
287 layers, reflecting the prevalence of high salinities in relatively deep summertime mixed layers,
288 and relatively low salinities (but much colder temperatures) in deep wintertime mixed layers.
289

290 Examination of the late-winter mixed layer properties sorted (and smoothed) as a function of
291 mixed layer depth (weighted by distance, time, and depth difference from the grid point) is
292 illuminating. In the Labrador Sea in mid-March, a substantial portion of the mixed layer depths
293 is relatively shallow, with a smaller portion of very deep values (Figure 3a). Hence, the
294 distribution is non-normal with a median value substantially less than the mean value, a
295 skewness of 0.59 (positive, so a stronger tail of deep values) and a kurtosis of 1.95 (< 3.0 , so
296 relatively light tails). Shallower (5th percentile) mixed layer depths are associated with colder
297 (Figure 3e) and fresher (Figure 3i) conditions, and deeper (95th percentile) mixed layer depths are
298 near average in temperature and saltier than average. In the EDW formation region in March, the
299 mean mixed layer depth (Figure 3b) is again larger than the median value, with a skewness of
300 0.53 (again, a stronger tail of deep values) and a kurtosis of 2.08 (again, light tails relative to a
301 normal distribution of 3). Shallower mixed layer depths are again associated with colder (Figure
302 3f) and fresher (Figure 3j) conditions, and deep mixed layers with colder and saltier than average
303 conditions. In the subantarctic southeast Pacific in mid-September, the mean and median mixed
304 layer depths (Figure 3c) are quite similar, with a skewness of 0.07 (a faintly stronger tail of deep
305 values) and a kurtosis of 2.90 (very close to the value of 3 for normal tails). Those values are
306 consistent with a depth distribution that is very close to normal, as is visually apparent. The very
307 shallowest mixed layers are associated with colder (Figure 3g) and saltier (Figure 3k) conditions,
308 which is puzzling, whereas deeper mixed layers are more intuitively associated with near-mean

309 temperatures, but saltier than mean conditions. Finally, in the core of the SPESTMW formation
310 region, the mid-September mean mixed layer depth value (Figure 3d) is slightly larger than the
311 median, with a skewness of 0.24 (a slightly stronger tail of deep values) and a kurtosis of 1.86 (<
312 3, so weaker than normal tails). Here deeper mixed layers are associated with colder (Figure 3h)
313 and saltier (Figure 3l) conditions, and shallower mixed layers with warmer than average
314 temperatures and saltier than average salinities.

315

316 *3.3 Late Winter and Late Summer Mixed Layer Properties at 95th Percentile Depths*

317 Northern Hemisphere mixed layer values are deepest in late winter to early spring, generally
318 around mid-March. In that month mixed layer depth 95th percentile values (Figure 4a) exceed
319 1600 m in the Labrador and Greenland Seas, 566 m in the western subtropical North Atlantic,
320 and 400 m in the western subtropical North Pacific. They are less than 25 m in the eastern
321 equatorial Pacific, and only exceed 200 m in a few isolated regions of the Southern Ocean, being
322 less than 100 m deep across much of the subtropical Southern Hemisphere oceans during austral
323 late summer, although exceeding 100 m in the central tropical South Pacific, where trade winds
324 are strong.

325

326 The ratio of mean to 95th percentile depths in March (Figure 5a) is smaller (so 95th percentile
327 mixed layer depths are relatively deep compared to the mean values) in the Northern Hemisphere
328 than in the south, with generally smaller values (0.3 to 0.4) in the western subtropics than in the
329 tropics of that hemisphere. The subpolar North Pacific and Bering Sea have a relatively large
330 ratio in March, about 0.6 to 0.8, so 95th percentile mixed layer depths are not so much larger than
331 mean values. In contrast, in the center of the Labrador Sea of the subpolar North Atlantic, that

332 ratio dips below 0.2, so there 95th percentile mixed layer depths exceed mean values by a factor
333 of more than five. In the Southern Hemisphere the ratio generally increases poleward, being
334 about 0.4 near the equator, increasing to about 0.5 and 0.6 in the tropical Pacific and Indian
335 oceans, closer to 0.6 to 0.7 in the eastern subtropical Pacific and tropical South Atlantic. Within
336 and south of the Antarctic Circumpolar Current (ACC) the ratio exceeds 0.6 and even 0.8 in a
337 few isolated locations.

338

339 The temperatures and salinities for the 95th percentile mixed layer depths are not so different
340 from many other climatologies, so they are not discussed here. Instead, temperature and salinity
341 differences for the 95th percentile depths minus the mean mixed layer values of temperature and
342 salinities are discussed to reveal some of what is driving the variations in mixed layer depths.
343 Since the global average of the thermal expansion coefficient α to the haline contraction
344 coefficient β at the surface is about 0.4, these temperature differences are contoured at 0.5 °C
345 intervals and the salinity differences at 0.2 g kg⁻¹. Hence, in the subtropics one contour of salinity
346 difference is roughly equivalent in magnitude (although opposite in sign) with respect to the
347 effect on density of one contour of temperature difference. At higher latitudes the contouring
348 choice substantially overemphasizes the effect of temperature on density compared to salinity,
349 since α/β at higher latitudes can fall below 0.1. In the tropics the contouring choice slightly
350 underemphasizes the effect of temperature on density, since α/β can approach 0.5 there.

351

352 In March deep (95th percentile) mixed layers are generally warmer (Figure 6a) and saltier (Figure
353 7a) than mean mixed layer conditions in the western subpolar northwest Pacific, and
354 anomalously fresh and cool mixed layers are shallower, as expected in a predominantly salt-

355 stratified high-latitude pycnocline. In the eastern subpolar North Pacific and the Bering Sea the
356 deeper late winter mixed layers are also saltier but slightly cooler too. In the subtropical North
357 Pacific and North Atlantic deep mixed layers are cooler than the mean mixed layer values, but
358 tend toward fresher in the west and saltier in the east (where subsurface salinity is higher).
359 Around the edges of the Labrador Sea, east of Canada's Maritime Provinces and USA's New
360 England, and in the vicinity of the North Atlantic Current, deep mixed layers are generally
361 warmer and much saltier than mean mixed layer values, again reflecting the stratifying influence
362 of cold, fresh surface waters in the region. In the tropics, and very prominently in the Bay of
363 Bengal, deep mixed layers are generally slightly cooler, and saltier, again reflecting the
364 stratifying influence of shallow fresh surface mixed layers there. In the subtropical Southern
365 Hemisphere, deep March mixed layers are substantially cooler (and usually slightly saltier) than
366 mean mixed layers, likely reflecting the importance of insolation in creating shallow mixed
367 layers in winter, probably during calm conditions, as precipitation is relatively uncommon there.
368 At higher southern latitudes, deep March mixed layers are often warmer and saltier than mean
369 mixed layer properties, again reflecting the importance of freshwater near the surface in setting
370 the subpolar stratification.

371

372 In mid-September, 95th percentile mixed layer depths (Figure 4b) are deepest north of the
373 Subantarctic Front, exceeding 800 m south of Australia and New Zealand and in a very small
374 region of the Southeast Pacific. They exceed 400 m in a portion of the subtropical gyre in the
375 South Atlantic Ocean, and 283 m in the subtropical Southeast Pacific Ocean. In the Northern
376 Hemisphere, September mixed layer 95th percentile depths are generally shallower than 100 m,
377 except in small portions of the western subtropical North Pacific, the subpolar North Atlantic,

378 and again in the central tropical Pacific under the trade winds. In the Pacific they reach values
379 shallower than 35 m in isolated regions of the central North Pacific, south of Baja, west of
380 Central America, and the eastern equatorial Pacific. In the Atlantic in September the 95th
381 percentile mixed layer depth is shallower than 35 m east of the Amazon, and west of Africa on
382 both sides of the equator.

383
384 The ratio of 95th percentile to mean mixed layer depths in September (Figure 5b) in the Northern
385 Hemisphere subtropical and subpolar regions generally exceeds 0.5 or 0.6 (and in a few locations
386 of the subpolar North Pacific tops 0.7). This ratio is lower in the Arabian Sea, where it dips
387 below 0.4, consistent with some relatively deep mixed layers at the end of the Southwest
388 Monsoon season, but with more frequent shallower mixed layers as well. In the western portions
389 of the Southern Hemisphere subtropical regions the ratio drops to below 0.4 in places, and even
390 below 0.3 in the western South Atlantic, off Southeast Australia, and off South Africa. South of
391 the ACC the ratio exceeds values of 0.6 in many locations and 0.8 in some locations, so the mean
392 and 95th percentile depths are not so different in this location in late winter or early spring (mid-
393 September).

394
395 In mid-September in the subpolar North Pacific and subpolar North Atlantic the temperatures at
396 mixed layer 95th percentile depths (Figure 6b) are substantially lower than the mean mixed layer
397 temperatures and corresponding salinity values (Figure 7b) are only slightly saltier. This is to be
398 expected since warmer shallower mixed layers will be prevalent in these months, punctuated by
399 colder, deeper, and saltier mixed layers during the first autumn storms. Moving south into the
400 subtropics deep (95th percentile) mixed layers appear associated with substantially saltier, but

401 only slightly colder mixed layers in the North Pacific, whereas in the interior of the subtropical
402 North Atlantic deep mixed layers in mid-September are substantially colder, but not much saltier
403 than the mean. Off the east coast of North America deep mixed layers are much saltier and
404 warmer, reflecting the correlation of cold, fresh, subpolar waters with shallower mixed layers in
405 that region. In the tropics of all three oceans, deep mixed layers are saltier, but generally not
406 much different in temperature from the mean values, reflecting the association of fresh surface
407 conditions with shallower mixed layers. This pattern includes the Bay of Bengal and east of the
408 Amazon, where shallow fresh mixed layers of riverine influence may also be prevalent. The one
409 exception in terms of mixed layer temperatures in the tropical band is the eastern equatorial
410 Pacific, where deep mixed layers are also substantially warmer. This occurs because in this
411 region upwelling cold waters are generally associated with shallower mixed layers, and deep
412 warmer mixed layers can more easily form when or where that upwelling is not present. In the
413 Southern Hemisphere subtropics there is not a clear large-scale pattern of temperature or salinity
414 with deep mixed layers. However, just north of the ACC, deep mixed layers are generally colder
415 and fresher in the Atlantic and Indian oceans, but colder and slightly saltier in the Pacific Ocean
416 in mid-September. Within the ACC, deep mixed layers are substantially warmer and saltier in the
417 Atlantic and Indian oceans, and substantially warmer but only a bit saltier in the Pacific Ocean.
418 This pattern reflects the association of cold and fresh Antarctic waters with shallower mixed
419 layers in these regions, and the relatively fresh subsurface waters in the Pacific compared to the
420 other oceans. South of the ACC deep mixed layers are generally substantially warmer, but only
421 slightly saltier.

422

423 *3.4. Skewness and Kurtosis of Mixed Layer Properties*

424 Mixed layer depth skewness and kurtosis are both strongest in the transitions between spring and
425 summer, when very shallow mixed layers often form but much deeper mixed layers are
426 occasionally still present. In mid-May, skewness (Figure 8a) exceeds +1 in most of the Northern
427 Hemisphere, and is often higher, even exceeding +3, in small portions of the North Atlantic
428 Current, the Labrador Sea, and the Greenland-Iceland-Norwegian (GIN) Sea. In all these regions
429 with positive skewness, the tail of the deep mixed layer values is strong, consistent with
430 prevalence of shallower values in times of restratification, punctuated by a few much deeper
431 values which constitute that strong tail. In the Southern Hemisphere in mid-May, skewness is
432 generally negative, but only falls below -1 or -2 in a few small regions. Hence, while deeper
433 mixed layers are favored in this time period, shallower mixed layers are also not infrequent.
434 Kurtosis in mid-May (Figure 9a) is generally high when skewness is high or low, so mixed layer
435 depth tails are generally stronger when the distribution is either positive or negatively skew in
436 that month. Hence, kurtosis is higher than normal ($> +3$, and indeed $> +5$ and much more in
437 many locations) in much of the extratropical Northern Hemisphere in mid-May where skewness
438 is positive and large, and kurtosis is also high in smaller portions of the Southern Ocean where
439 skewness is large and of either sign. Kurtosis is almost never $< +1$ in this month.

440

441 In November mixed layer depth skewness (Figure 8b) is positive throughout much of the
442 Northern Hemisphere tropics and almost all of the Southern Hemisphere. It exceeds +1 in many
443 Southern Hemisphere locations, and exceeds +2 in some parts of the ACC. It is also mildly
444 positive in much of the subpolar North Atlantic and the GIN Sea. Hence, shallow mixed layer
445 depths are more prevalent in these locations, with more infrequent deep mixed layers on the
446 positive side of the distribution. Mixed layer depth skewness is mildly negative in most of the

447 subtropical North Pacific and North Atlantic, and most of the Subpolar North Pacific as well.
448 However, it is less than -1 in only very limited scattered regions. Kurtosis in mid-November
449 (Figure 9b) exceeds +3 along the equator in much of the Southern Hemisphere subtropics, and
450 exceeds +5 in smaller areas of these regions, but it is highest in the ACC, where mixed layer
451 depth tails are large (and positively skewed). So, in this transition month in the ACC, shallower
452 mixed layer values are prevalent, but there are strong positive tails because of a few much deeper
453 values. Kurtosis in mid-November is $< +3$ in large portions of the Northern Hemisphere
454 subtropical gyres, in the tropics (excepting the equator), and south of the ACC, but it is never
455 $< +1$. So, in these regions in mid-November the tails are weaker than they would be for a normal
456 distribution.

457

458 Regional patterns in mixed layer temperature skewness and kurtosis (not shown) are generally
459 not as striking as those for mixed layer depth. Mixed layer temperature is strongly positively
460 skew with high kurtosis around Antarctica in the austral winter through spring because most
461 mixed layer temperatures are near the freezing point of seawater, so any warmer values that are
462 present create a strong positive tail. In addition, there is strong negative skewness and strong
463 positive kurtosis in winter and spring off the east coast of North America, probably owing to
464 occasional offshore sampling of cold high latitude water masses usually found near the coast.
465 Mixed layer salinity distributions exhibit large negative skewness and high kurtosis in that same
466 region, present year-round, owing to the freshness of these same high latitude water masses.
467 There is also considerable structure in salinity skewness north of much of the ACC, with bands
468 of positive and negative skewness, each associated with high kurtosis, and low kurtosis between
469 them. This pattern is especially prominent in the Indian Ocean sector of the Southern Ocean,

470 where conditions in the northern negative skew band are on the whole relatively salty but
471 occasional fresh conditions create strong tails, and conditions in the negative skew band to the
472 south are on the whole relatively fresh but occasional salty conditions favor strong tails. Some of
473 this pattern may be local and temporal, but some is very likely to be spatial, a result of the ~500
474 km length-scale used in the weighting extending across fronts.

475

476 **4. Summary**

477 We constructed a global monthly mixed layer climatology by applying the *Holte and Talley*
478 (2009) density algorithm to Argo data and putting the mixed layer depths, conservative
479 temperatures, and absolute salinities obtained on a grid using a weighting of nearby data
480 considering differences of location, time, and bottom depth between the data and the grid points.
481 In addition to computing weighted means, variances, skewness, and kurtosis for these properties
482 at each grid point at each month, we sorted by all three variables by mixed layer depth, weighted
483 them all in terms of distance, time, and depth difference from the grid point, and then smoothed
484 all three depth-sorted variables to find values at the 5th, 50th, and 95th percentiles of mixed layer
485 depth.

486

487 The mean number of data points used for each grid point is 122, although there is substantial
488 spatial variability (Figure 1a). Since the sum of the weights for the grid points is on average
489 about $\frac{1}{4}$ of the sum of the number of samples used at each grid point, the mean sum of the
490 weights is 30, again with spatial variability (Figure 1b).

491

492 Seasonal cycles (Figure 2) of 5th, 50th, 95th, and mean values of depth, temperature, and salinity
493 at the centers of four mode water formation regions (one each in the subtropics and subpolar
494 regions of each hemisphere) reveal the striking asymmetry where seasonally mixed layers
495 deepen more slowly during the fall than they do in spring. They also show that in a few locations
496 and times the 95th percentile depth values can exceed mean values by a factor of five or more.
497 Additionally, sometimes the median mixed layer properties can differ substantially from the
498 mean values. Late winter mixed layer depths at 95th percentiles can be more than three times the
499 mean values in some regions (Figure 5), but there is again considerable spatial variability. Late
500 winter temperatures of the 95th percentile depth mixed layers (Figure 6) are often lower than
501 mean mixed layer temperatures in the subtropics, and late winter salinities of the 95th percentile
502 depth are often higher than the means in the subpolar regions and portions of the tropics. These
503 patterns are consistent with the importance of temperature in upper ocean stratification in the
504 subtropics and salinity in the subpolar regions. While mixed layer depth distributions are rarely
505 close to normal, they tend to be most skew (Figure 8) with the highest kurtosis (Figure 9) in the
506 spring transition months of May (in the Northern Hemisphere) and September (in the Southern
507 Hemisphere), when frequent shallow mixed layer depths are punctuated by occasional deep
508 mixed layers.

509

510 The monthly climatological values for mixed layer depth, temperature, and salinity we make
511 available (at <https://www.pmel.noaa.gov/gosml>) include the usual means and variances. In
512 addition, skewness and kurtosis allow assessment of how non-normal the variable distributions
513 are in a given location and month of the year. Values of temperature, salinity, and depth at the
514 5th, 50th, and 95th percentiles of mixed layer depth are useful for studying the mixed layer under a

515 variety of states. First, the 95th percentile values are of interest as they are representative of
516 ventilated conditions, robust to extreme outliers and more statistically uniform than the average
517 of the three deepest samples in a bin (Holte et al., 2017). The 50% values may be useful as
518 alternatives to, or for comparison with the mean values, since mixed layer property distributions
519 are often non-normal. Those interested in the ocean state when mixed layers are shallow may
520 find the 5th percentile values of use. Finally, the differences between the 5th and 95th percentile
521 values give alternative indicators of the ranges of conditions experienced in a given month and
522 location, perhaps better suited than the mean and variance for non-normal distributions.

523

524 **Acknowledgments and Data Availability Statement**

525 This work was supported by the NOAA Global Ocean Monitoring and Observation Program, and
526 NOAA Research. The data used for this study were collected and made freely available by the
527 International Argo Program and the national programs that contribute to it
528 (<https://dx.doi.org/10.17882/42182>). The GOSML climatology is freely available at
529 <https://www.pmel.noaa.gov/gosml>. PMEL Contribution Number 5294.

530

531 **References**

- 532 Billheimer, S., & Talley, L. D. (2016). Annual cycle and destruction of Eighteen Degree Water.
533 *Journal of Geophysical Research: Oceans*, 121(9), 6604–6617.
534 <https://doi.org/10.1002/2016jc011799>
- 535 Boccaletti, G., Ferrari, R., & Fox-Kemper, B. (2007). Mixed layer instabilities and
536 restratification. *Journal of Physical Oceanography*, 37(9), 2228–2250.
537 <https://doi.org/10.1175/jpo3101.1>

538 Cleveland, W. S., & Devlin, S. J. (1988). Locally weighted regression - an approach to
539 regression-analysis by local fitting. *Journal of the American Statistical Association*,
540 83(403), 596–610. <https://doi.org/10.2307/2289282>

541 Damerell, G. M., Heywood, K. J., Calvert, D., Grant, A. L. M., Bell, M. J., & Belcher, S. E.
542 (2020). A comparison of five surface mixed layer models with a year of observations in
543 the North Atlantic. *Progress in Oceanography*, 187, 102316.
544 <https://doi.org/10.1016/j.pocean.2020.102316>

545 de Boyer Montegut, C., Madec, G., Fischer, A. S., Lazar, A., & Iudicone, D. (2004). Mixed layer
546 depth over the global ocean: An examination of profile data and a profile-based
547 climatology. *Journal of Geophysical Research: Oceans*, 109, C12003.
548 <https://doi.org/10.1029/2004jc002378>

549 Feistel, R. (2012). TEOS-10: A New International Oceanographic Standard for Seawater, Ice,
550 Fluid Water, and Humid Air. *International Journal of Thermophysics*, 33(8–9), 1335–
551 1351. <https://doi.org/10.1007/s10765-010-0901-y>

552 Holte, J., & Talley, L. (2009). A New Algorithm for Finding Mixed Layer Depths with
553 Applications to Argo Data and Subantarctic Mode Water Formation. *Journal of*
554 *Atmospheric and Oceanic Technology*, 26(9), 1920–1939.
555 <https://doi.org/10.1175/2009jtecho543.1>

556 Holte, J., Talley, L. D., Gilson, J., & Roemmich, D. (2017). An Argo mixed layer climatology
557 and database. *Geophysical Research Letters*, 44(11), 5618–5626.
558 <https://doi.org/10.1002/2017GL073426>

559 Johnson, G. C., S. Hosoda, S. R. Jayne, P. R. Oke, S. C. Riser, D. Roemmich, T. Suga, V.
560 Thierry, S. E. Wijffels, and J. Xu. (2022). Argo—Two Decades: *Global Oceanography*,

561 Revolutionized. *Annual Review of Marine Science*, 14:379–403. doi:/10.1146/annurev-
562 marine-022521-102008.

563 Kara, A. B., Rochford, P. A., & Hurlburt, H. E. (2003). Mixed layer depth variability over the
564 global ocean. *Journal of Geophysical Research-Oceans*, 108(C3), 3079.
565 <https://doi.org/10.1029/2000jc000736>

566 Price, J. F., Weller, R. A., & Pinkel, R. (1986). Diurnal cycling - observations and models of the
567 upper ocean response to diurnal heating, cooling, and wind mixing. *Journal of*
568 *Geophysical Research-Oceans*, 91(C7), 8411–8427.
569 <https://doi.org/10.1029/JC091iC07p08411>

570 Rao, R. R., & Sivakumar, R. (2003). Seasonal variability of sea surface salinity and salt budget
571 of the mixed layer of the north Indian Ocean. *Journal of Geophysical Research-Oceans*,
572 108(C1), 3009. <https://doi.org/10.1029/2001jc000907>

573 Sallée, J. B., Speer, K., Rintoul, S., & Wijffels, S. (2010). Southern Ocean Thermocline
574 Ventilation. *Journal of Physical Oceanography*, 40(3), 509–529.
575 <https://doi.org/10.1175/2009jpo4291.1>

576 Smith, W. H. F., & Sandwell, D. T. (1997). Global sea floor topography from satellite altimetry
577 and ship depth soundings. *Science*, 277(5334), 1956–1962.
578 <https://doi.org/10.1126/science.277.5334.1956>

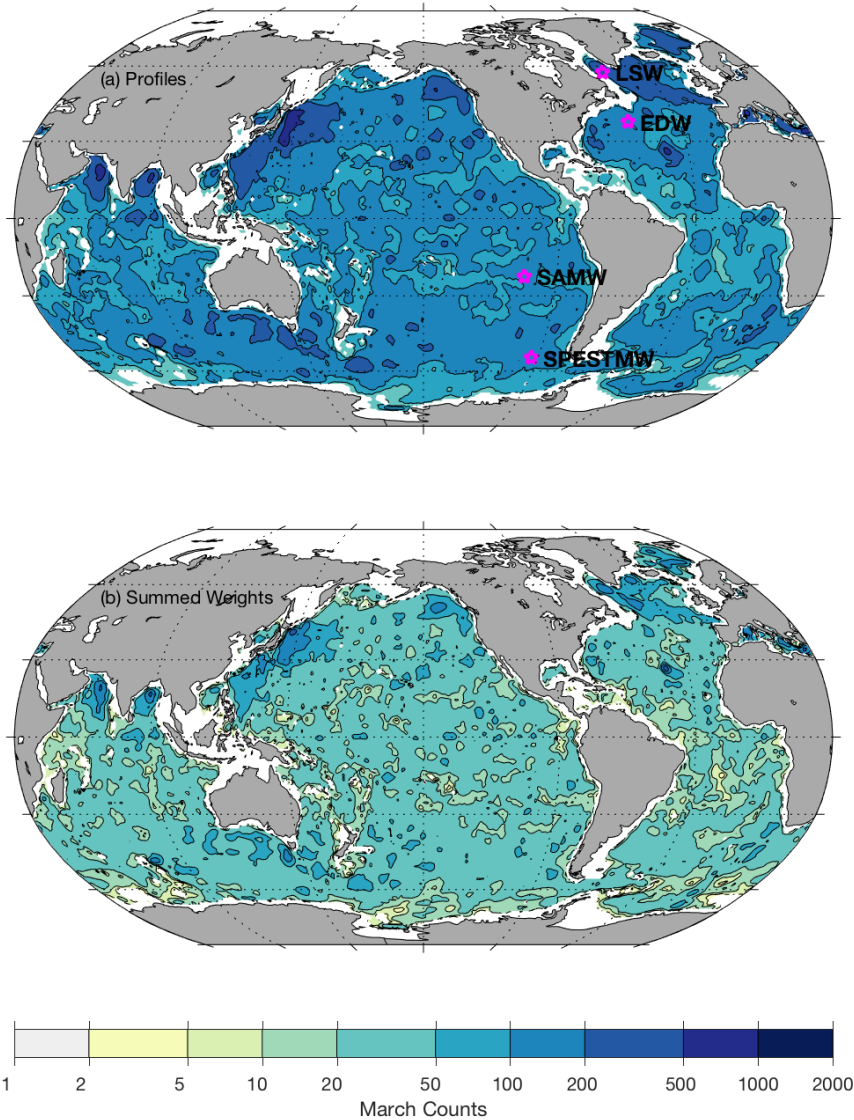
579 Sprintall, J., & Tomczak, M. (1992). Evidence of the barrier layer in the surface-layer of the
580 tropics. *Journal of Geophysical Research-Oceans*, 97(C5), 7305–7316.
581 <https://doi.org/10.1029/92jc00407>.

582 Vernet, M., Martinson, D., Iannuzzi, R., Stammerjohn, S., Kozlowski, W., Sines, K., Smith, R.,
583 and Garibotti, I. (2008). Primary production within the sea-ice zone west of the Antarctic

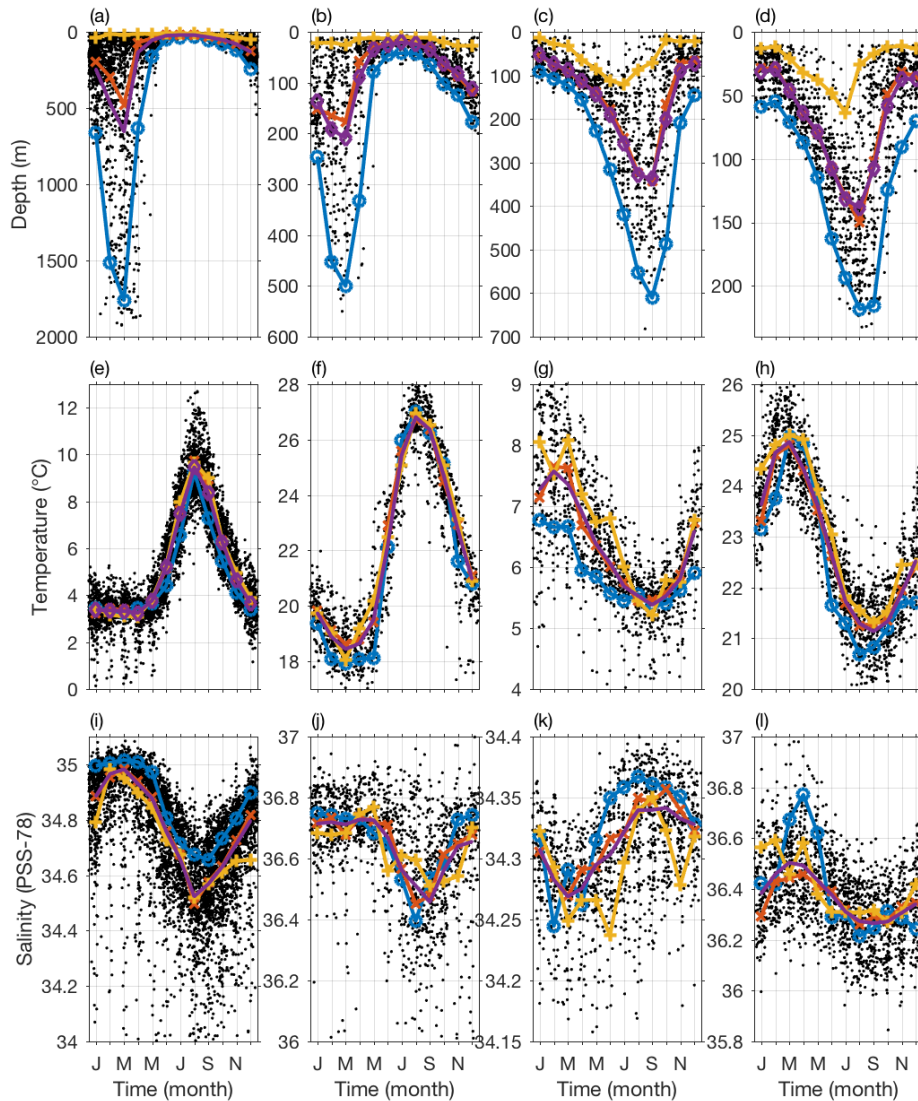
584 Peninsula: I-Sea ice, summer mixed layer, and irradiance. *Deep-Sea Research Part II-*
585 *Topical Studies in Oceanography*, 55(18–19), 2068–2085.
586 <https://doi.org/10.1016/j.dsr2.2008.05.021>

587 Wong, A. P. S., & Johnson, G. C. (2003). South Pacific Eastern Subtropical Mode Water.
588 *Journal of Physical Oceanography*, 33(7), 1493–1509. [https://doi.org/10.1175/1520-](https://doi.org/10.1175/1520-0485(2003)033<1493:spesmw>2.0.co;2)
589 [0485\(2003\)033<1493:spesmw>2.0.co;2](https://doi.org/10.1175/1520-0485(2003)033<1493:spesmw>2.0.co;2)

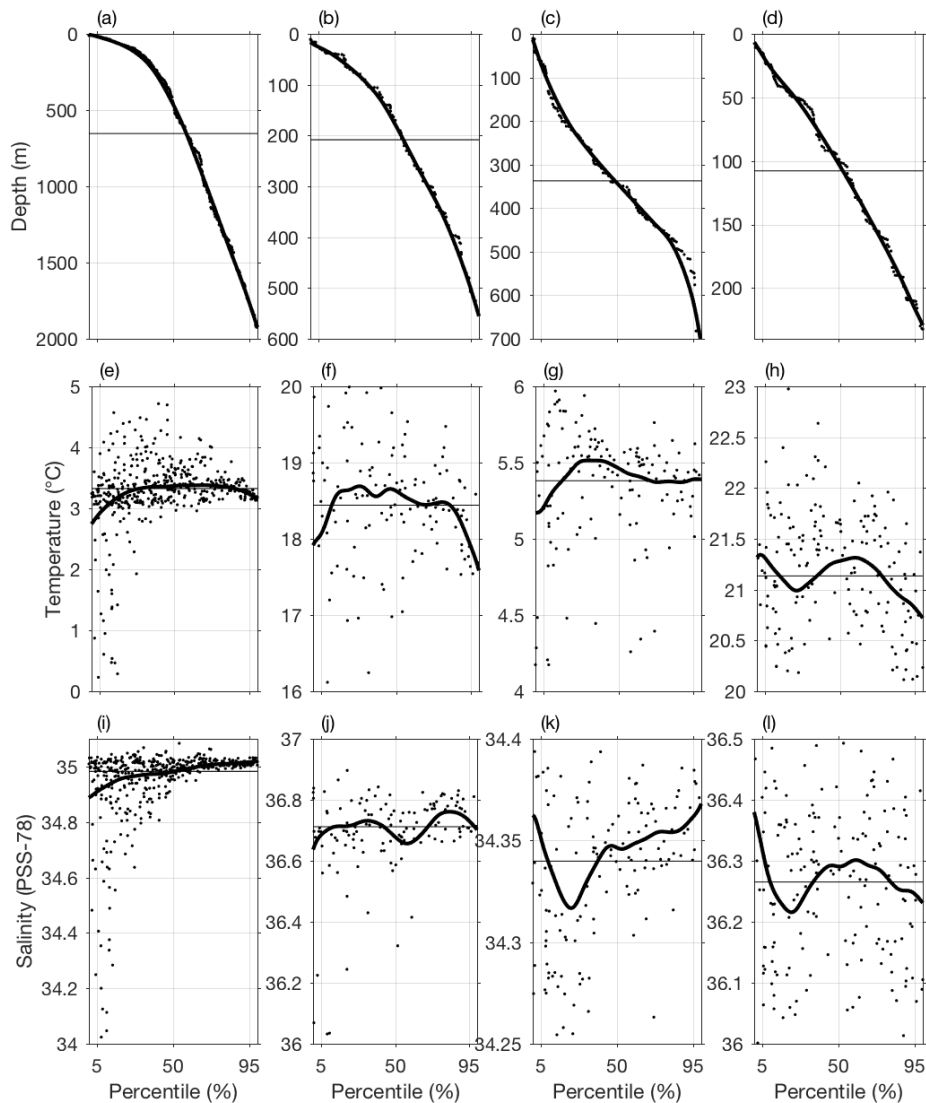
590 Yashayaev, I., & Loder, J. W. (2016). Recurrent replenishment of Labrador Sea Water and
591 associated decadal-scale variability. *Journal of Geophysical Research-Oceans*, 121(11),
592 8095–8114. <https://doi.org/10.1002/2016jc012046>



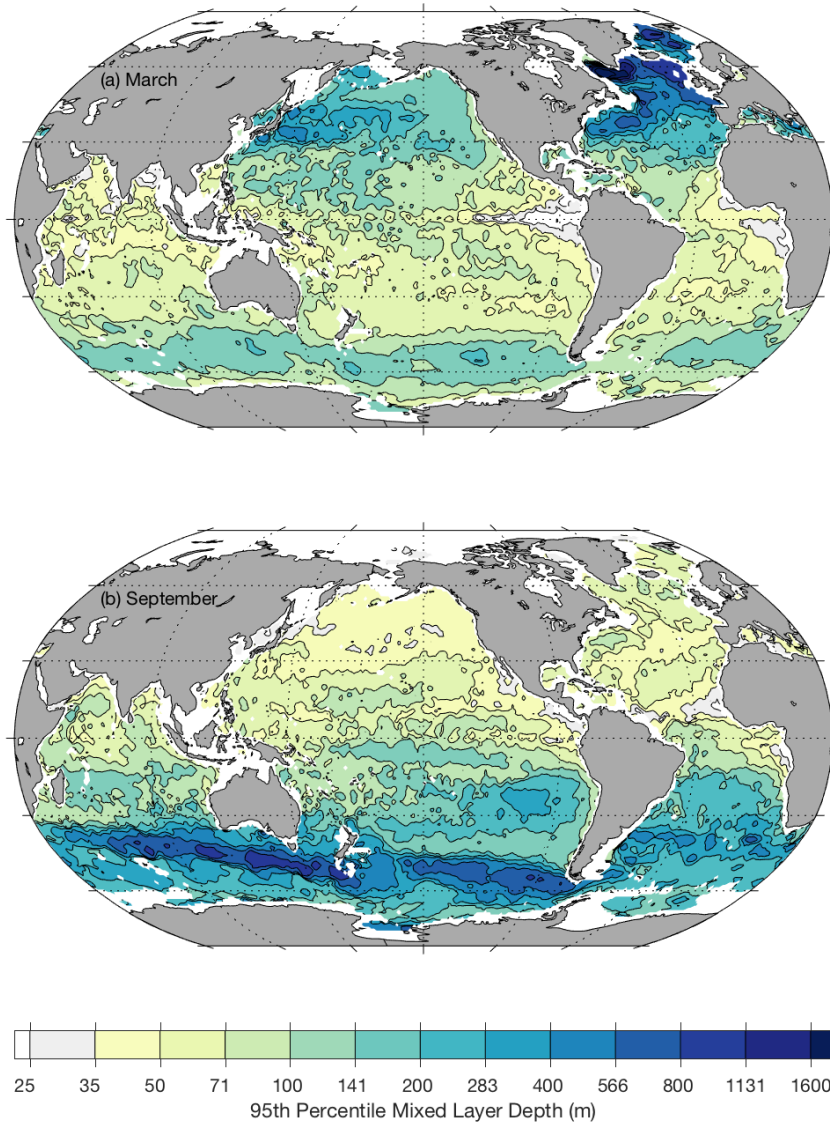
594 **Figure 1.** (a) Number of profiles used at each grid point and (b) sum of weights for profiles for
 595 the mid-March maps contoured at roughly logarithmic intervals (see colorbar). Formation
 596 regions (magenta pentagrams in a) for mode waters at which the seasonal cycles of mixed layer
 597 properties and late winter mixed layer property distributions are examined include, from north to
 598 south: Labrador Sea Water (LSW), Eighteen Degree Water (EDW), South Pacific Eastern
 599 SubTropical Mode Water (SPESTMW), and SubAntarctic Mode Water (SAMW) in the
 600 southeastern Pacific Ocean.



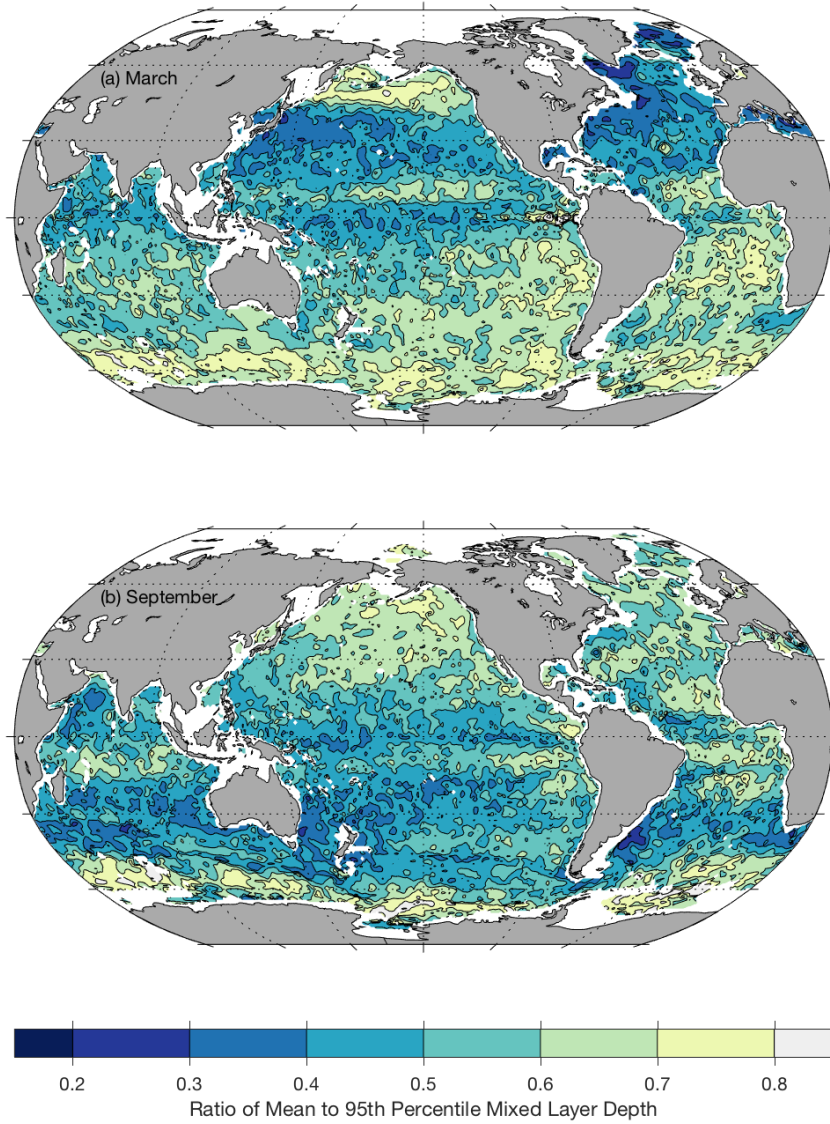
603 **Figure 2.** Seasonal cycles of mixed layer depths (top row), conservative temperature (middle
 604 row), and salinity (bottom row) for LSW (far left column), EDW (middle left column),
 605 SPESTMW (middle right column), and SAMW (far right column) in the southeastern Pacific
 606 Ocean (see magenta pentagrams in Figure 1a for locations). Raw values (black dots), mapped
 607 monthly values corresponding to 95th percentile mixed layer depths (blue line with circles), 50th
 608 percentile mixed layer depths (orange line and crosses), 5th percentile mixed layer depths (yellow
 609 line and plusses), and mean values (purple line and diamonds) are shown.



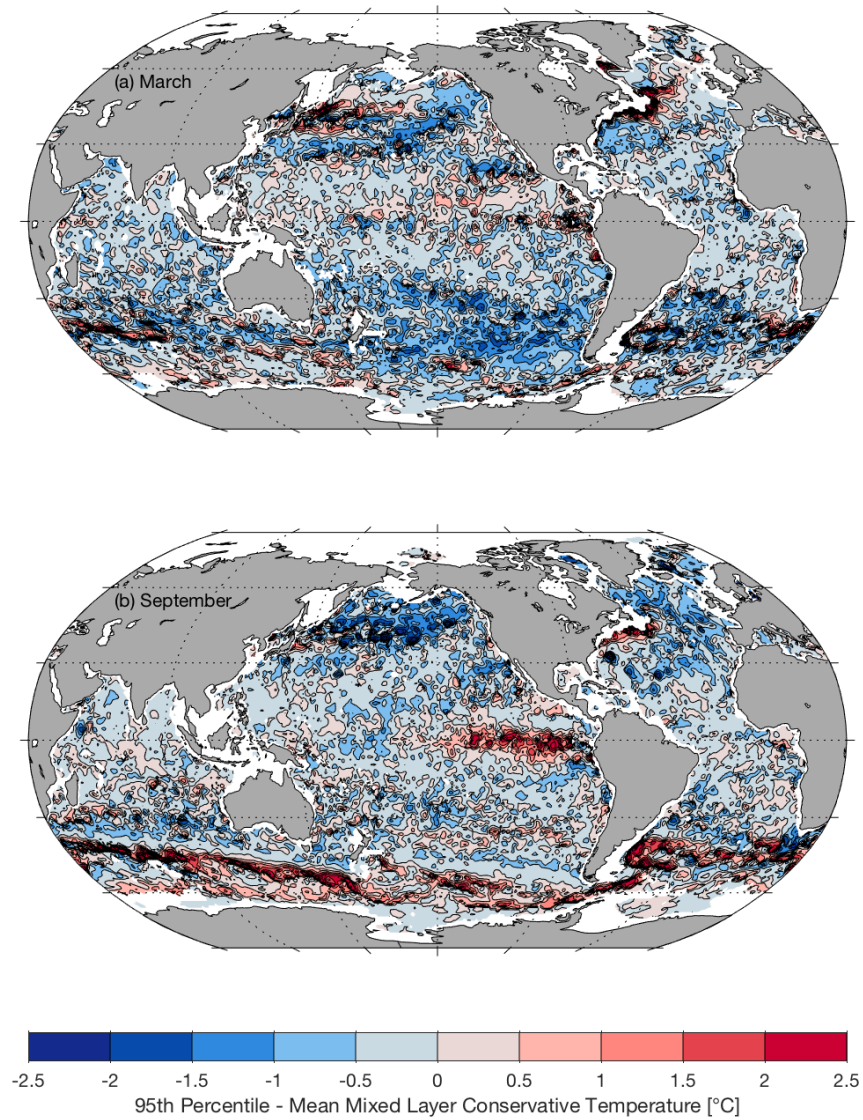
612 **Figure 3.** Late winter mixed layer depth (top row), conservative temperature (middle row), and
 613 salinity (bottom row) distributions for LSW (far left column) and EDW (middle left column) in
 614 mid-March, as well as SPESTMW (middle right column) and SAMW (far right column) in the
 615 southeastern Pacific Ocean in mid-September (see magenta pentagrams in Figure 1a for
 616 locations). Raw values (black dots) sorted by mixed layer depth and weighted by distance, time,
 617 and depth separation from the grid point, and lowess smoothed values for those properties using
 618 a length scale of 25% (black lines) are shown.



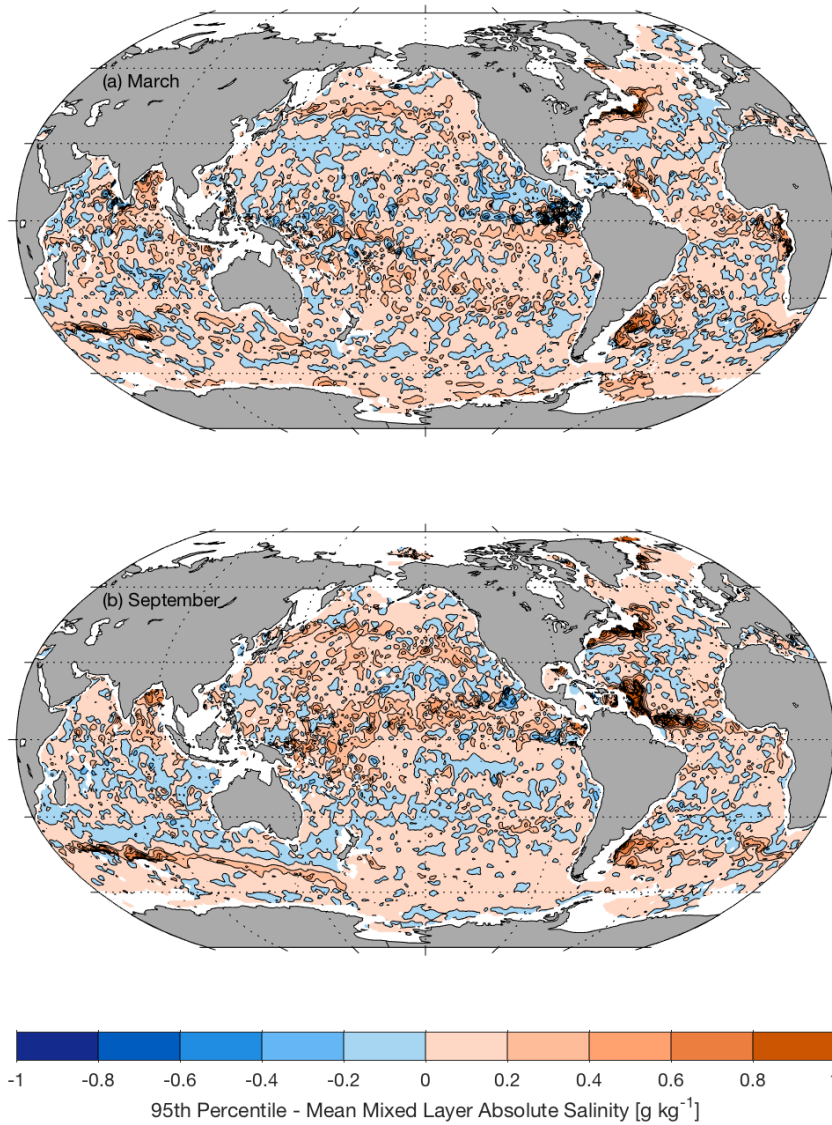
621 **Figure 4.** (a) Mid-March and (b) mid-September 95th percentile mixed layer depths contoured on
622 a logarithmic scale (colorbar) from 25 to 1600 m.



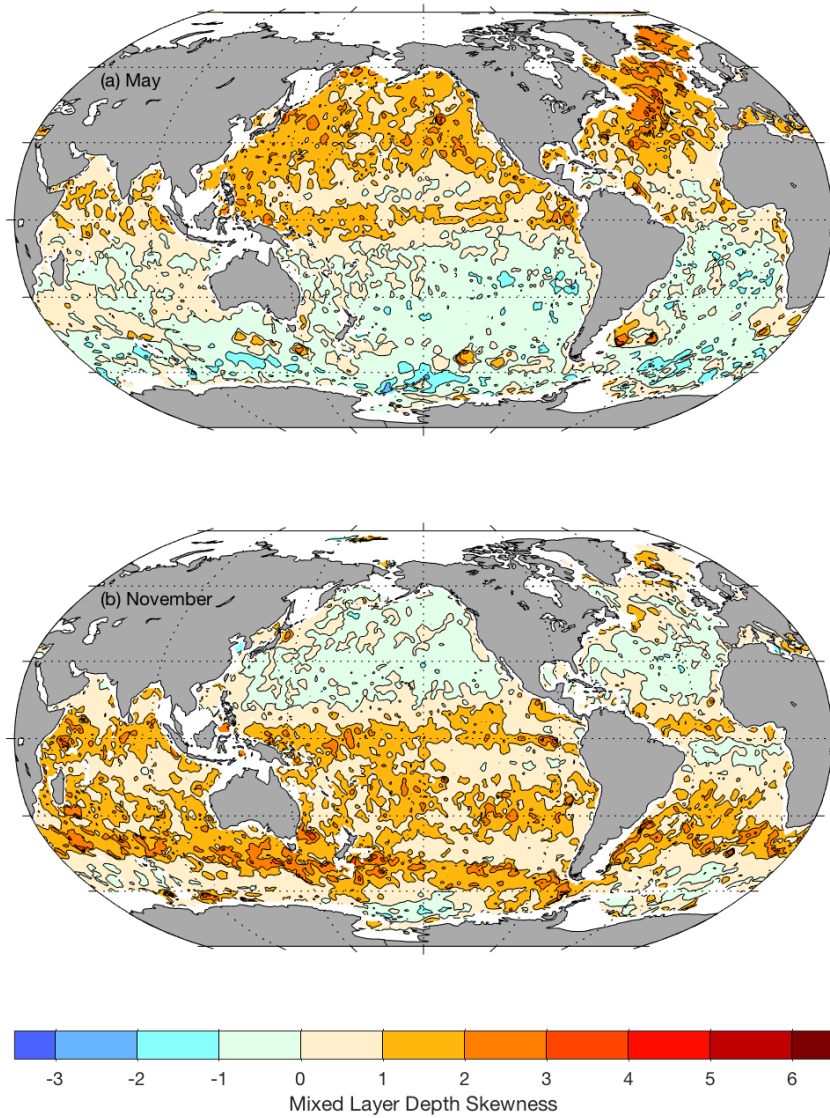
625 **Figure 5.** (a) Mid-March and (b) mid-September ratios of mean to 95th percentile mixed layer
626 depths contoured at 0.1 intervals (colorbar).



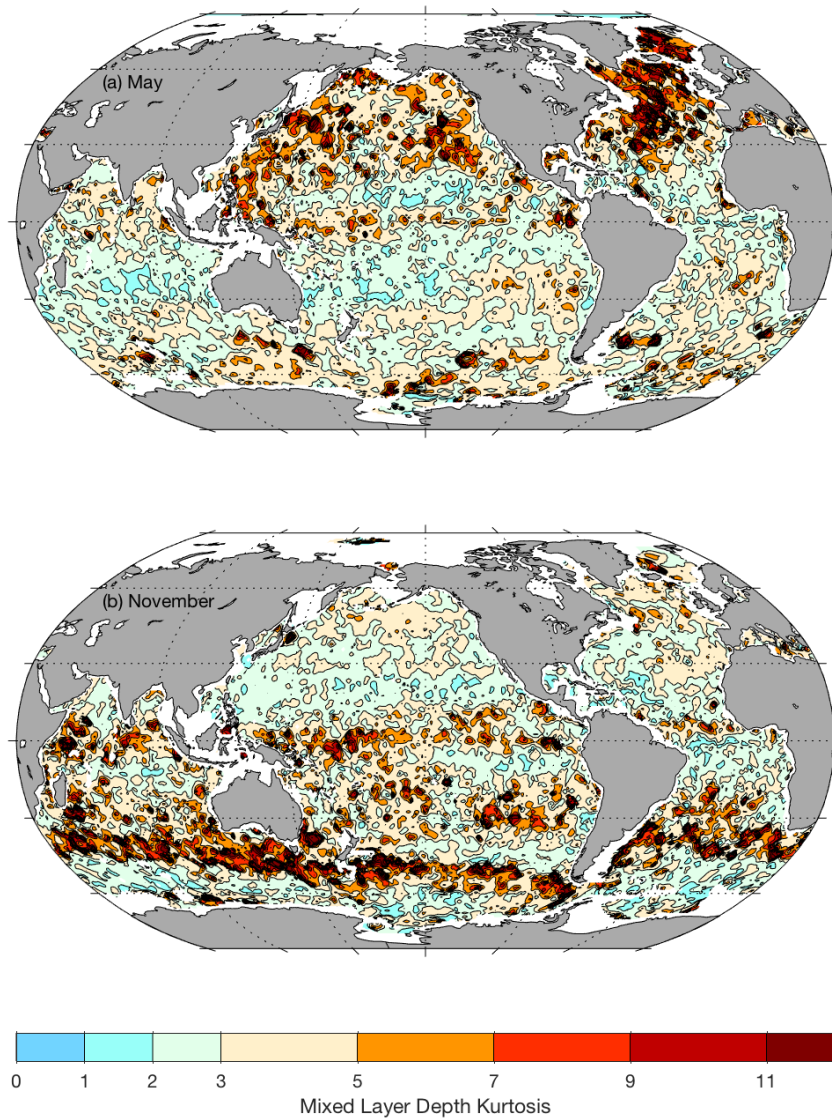
629 **Figure 6.** (a) Mid-March and (b) mid-September differences of conservative temperature for the
630 95th percentile mixed layer depth minus the mean mixed layer temperature contoured at 0.5 °C
631 intervals (colorbar).



634 **Figure 7.** (a) Mid-March and (b) mid-September differences of absolute salinity for the 95th
635 percentile mixed layer depth minus the mean mixed layer absolute salinity contoured at 0.2 g kg^{-1}
636 intervals (colorbar).



639 **Figure 8.** (a) Mid-May and (b) mid-November mixed layer depth distribution skewness
640 (colorbar). Positive values (yellow to red) indicate a strong tail of deeper mixed layer values, and
641 negative values (green to blue) indicate a strong tail of shallower mixed layer values.



644 **Figure 9.** (a) Mid-May and (b) mid-November mixed layer depth distribution kurtosis (colorbar).
645 Values exceeding three (yellow to red) indicate that mixed layer depth tails are stronger than for
646 a normal distribution and values less than three (green to blue) indicate that mixed layer depth
647 tails are weaker than for a normal distribution.